18TH WORLD CONFERENCE ON EARTHQUAKE ENGINEERING
WCEE2024
MILAN

MILAN, ITALY
30TH JUNE - 5TH JULY 2024
www.wcee2024.it

NATIONWIDE EARTHQUAKE RISK MODEL FOR MASONRY BUILDINGS IN MALAWI

K. Goda[1], J. Williams, R. De Risi, & I. Ngoma

[1] Western University, London, Canada, kgoda2@uwo.ca

[2] University of Otago, New Zealand, jack.williams@otago.ac.nz

[3] University of Bristol, United Kingdom, raffaele.derisi@bristol.ac.uk

[4] University of Malawi, The Polytechnic, Blantyre, Malawi, ingoma@poly.ac.mw

Abstract: This study develops a nationwide seismic risk model for masonry houses in Malawi by focusing on the collapse limit state. The new seismic risk model reflects the latest seismic hazard characterization of active faults in the southern segment of the East African Rift system and country-specific collapse fragility functions that are derived based on local building surveys, experimental tests of local construction materials, and plausible failure mechanisms of the main structural elements of the Malawian houses. Overall, the new quantitative seismic risk model significantly improves existing seismic risk assessment tools without country-specific hazard-exposure-vulnerability models. The collapse risk curves are evaluated on a national scale by utilizing the advantage brought by the upper tail approximation method of site-specific seismic hazard curves. The results are useful for emergency managers and policymakers for nationwide seismic risk management purposes.

1. Introduction

Risk-informed decision-making is the key to efficiently allocating and using resources for disaster risk management. For low-to-middle-income countries that are exposed to earthquakes, accessibility to quantitative seismic risk decision-support tools is limited. This is particularly important for Eastern African countries, where available seismic data and models are lacking, building and population exposure models are incomplete, and appropriate seismic vulnerability models have not been developed. In this regard, the Global Earthquake Model Foundation (https://www.globalquakemodel.org/gem) has contributed significantly by developing open-source seismic hazard and risk models. However, their model details are not sufficiently detailed to capture country-specific characteristics of hazard, exposure, and vulnerability models (Poggi et al., 2017).

Malawi is one of the least developed countries in Eastern Africa and is prone to earthquakes with vulnerable constructions. Due to its position within the East African Rift system, earthquakes with moderate moment magnitudes (M_w) occur (e.g., 1989 M_w 6.3 Salima earthquake and 2009 M_w 6.0 Karonga sequence). The areas around Lake Malawi and along the Shire River are surrounded by border and intra-basin faults, which are capable of generating M_w 7+ earthquakes (Flannery and Rosendahl, 1990; Jackson and Blenkinsop, 1997; Wedmore et al., 2020). The population in Malawi is concentrated in these areas with active seismicity (e.g., Blantyre, Zomba, Salima, Mzuzu, and Karonga), except for the capital city Lilongwe. Low-rise masonry buildings are the most prevalent construction type and are not seismically resistant (Kloukinas et al., 2020). Due to high seismic vulnerability under moderate shaking conditions (e.g., peak ground acceleration (PGA) less than 0.2 *g*), the potential impact of earthquakes can be very damaging to the country. Such nationwide seismic risk assessments have not been conducted for Malawi by adopting country-specific hazard-exposure-vulnerability information.

This study presents the most recent development of a nationwide earthquake risk model for masonry buildings in Malawi. As part of the *PREPARE* (enhancing *PREP*aredness for *E*ast *A*frican countries through seismic *R*esilience *E*ngineering) project (2016–2022), a new probabilistic seismic hazard analysis (PSHA) model has

been developed by taking into account fault-based seismic sources, in addition to conventional areal sources (Williams et al., 2023). The most recent 2018 national census data (National Statistical Office of Malawi, 2018) provide more accurate exposure information for Malawian people and their assets at detailed spatial resolutions (Goda et al., 2022). From seismic fragility assessment viewpoints, building surveys and experimental tests of local construction materials and wall panels have been conducted (Kloukinas et al., 2020; Voyagaki et al., 2020), and new seismic vulnerability functions have been derived (Novelli et al., 2021). By integrating these recent improvements in seismic hazard, exposure, and vulnerability modules, a quantitative seismic risk model for Malawi is developed on a national scale. An efficient statistical approach for approximating the upper tail distribution of a seismic hazard curve, which can be considered as an improvement of a power function approximation proposed by Cornell et al. (2002), is implemented for the rapid computation of seismic risk curves at individual locations. Using this technique, a seismic risk curve for a single location can be obtained very quickly (typically, less than a few seconds, depending on the simulation length); thereby, this can be easily expanded to the whole country with reasonable computational times. The results from this new quantitative decision-support tool will allow the calculations of annual expected losses for the entire country and provide a sound basis for science-based and risk-informed policies for disaster risk reduction in Malawi.

2. Earthquake Risk Model for Masonry Buildings in Malawi

A quantitative seismic risk assessment for masonry buildings in Malawi can be carried out by combining a seismic hazard module, building exposure module, and seismic vulnerability module and by considering uncertainties associated with these modules. Such risk assessments are often performed by generating stochastic event sets (consisting of numerous earthquake scenarios), simulating shaking intensity values for individual events, and evaluating seismic damage severities for a building portfolio of interest (Mitchell-Wallace et al., 2017). The computational resources required for a full probabilistic seismic risk assessment over a wide area become critical. To circumvent this challenge, a seismic hazard curve, which is a plot of the seismic hazard parameter (e.g., PGA and spectral acceleration) as a function of annual frequency of exceedance, is approximated by a surrogate statistical model. This facilitates the quantitative seismic risk evaluations at numerous building locations. A computational procedure of the quantitative seismic risk assessment is shown in **Figure 1** for the case of Malawi. Brief explanations of the model components are provided in the following subsections.

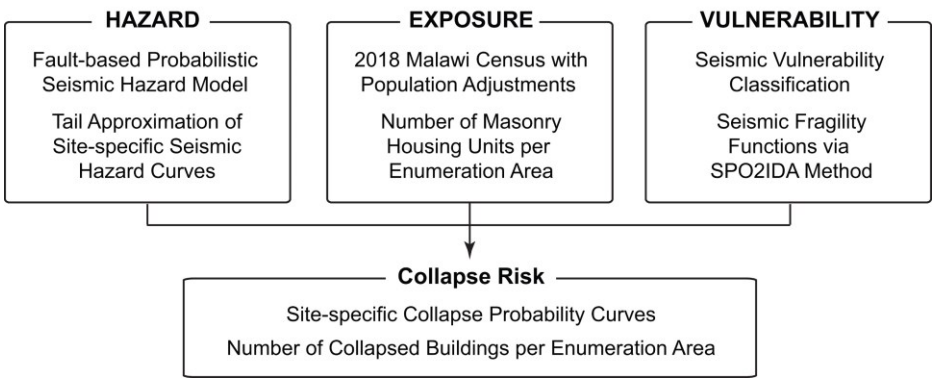

***Figure 1**. Seismic risk analysis procedure.*

2.1. Fault-based seismic hazard model and tail approximation of seismic hazard curves

The most recent PSHA model for Malawi considers both areal and fault sources (Williams et al., 2023). The areal sources are based on those for the East African Rift, defined by Poggi et al. (2017), whereas the fault sources are obtained from the Malawi Seismogenic Source Model (Williams et al., 2022). The considered fault sources are shown in **Figure 2a**; the faults are concentrated near Lake Malawi, and some border and intra-basin faults are inland. Five alternative source models are generated to reflect uncertainty for on-fault magnitude-frequency distributions. Since country-specific ground motion models are unavailable in Malawi, four ground motion models (GMM; Atkinson and Adams, 2013; Akkar et al., 2014; Boore et al., 2014; Chiou and Youngs, 2014) are considered in a logic tree. The Atkinson and Adams (2013) GMM is for the stable continental region; the Akkar et al. (2014) GMM is from the European SHARE project; and the Boore et al.

(2014) and Chiou and Youngs (2014) GMMs are from the NGA-West2 project. By combining 20 logic tree branches (i.e., five source models and four ground motion models) and taking PGA as a representative ground motion parameter (note: this choice is consistent with seismic fragility functions for masonry structures; Novelli et al., 2021), 20 ground motion values are calculated for the nine return periods 100, 200, 500, 750, 1,000, 2,000, 2,500, 5,000, and 10,000 years. **Figures 2b** and **2c** illustrate mean PGA maps at the return periods of 500 and 1,000 years. The PGA maps incorporate site amplifications based on USGS's global V_{s30} data (Wald and Allen, 2007). The seismic hazards are higher at Karonga in northern Malawi and at Blantyre and Zomba in southern Malawi.

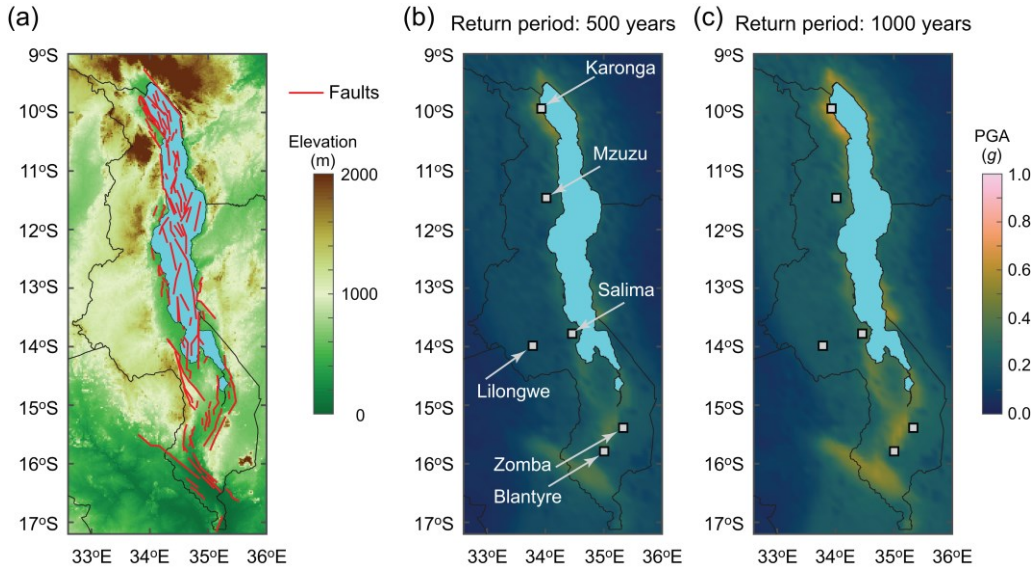

***Figure 2**. (a) Digital elevation model and finite faults near Lake Malawi (Williams et al., 2022). Peak ground acceleration maps at the return periods of 500 years (b) and 1,000 years (c) for Malawi (Williams et al., 2023).*

Utilizing the extracted seismic hazard values at the nine return period levels for individual locations, the upper-tail approximation of the PSHA results is carried out by plotting the data on different probability papers and identifying the most suitable probability distribution based on the least squares fitting. Four candidate distributions are considered, i.e., lognormal, Gumbel, Frechet, and Weibull. The horizontal and vertical plotting positions (x and y, respectively) of the lognormal, Gumbel, Frechet, and Weibull distributions are

Lognormal distribution: $$x = \ln(PGA) \text{ and } y = \Phi^{-1}(P) \quad (1)$$

Gumbel distribution: $$x = PGA \text{ and } y = -\ln(-\ln(P)) \quad (2)$$

Frechet distribution: $$x = \ln(PGA) \text{ and } y = -\ln(-\ln(P)) \quad (3)$$

Weibull distribution: $$x = \ln(PGA) \text{ and } y = \ln(-\ln(1-P)) \quad (4)$$

where ln represents the natural logarithm, P represents the cumulative probability, and $\Phi^{-1}(\bullet)$ represents the inverse standard normal distribution function. The linear correlation coefficient between the values from PSHA and the fitted model is used to select the most suitable model among the four candidates. Once the best-fit model is identified (i.e., probability distribution as well as intercept and slope of the fitted linear line $y = c_1 + c_2 \times x$), samples of the annual maximum PGA at a given site can be generated from

Lognormal distribution: $$PGA = \exp(-c_1/c_2 + (1/c_2) \times N(0,1)) \quad (5)$$

Gumbel distribution: $$PGA = -c_1/c_2 - \ln(-\ln(U(0,1)))/c_2 \quad (6)$$

Frechet distribution: $$PGA = \exp(-c_1/c_2 - \ln(-\ln(U(0,1)))/c_2) \quad (7)$$

Weibull distribution: $$PGA = \exp(-c_1/c_2 + \ln(-\ln(1-U(0,1)))/c_2) \quad (8)$$

where $N(0,1)$ is a standard normal random number, and $U(0,1)$ is a standard uniform random number.

Figure 3a shows the correlation coefficients between the PSHA data and the fitted upper tail approximation models at 18,714 seismic risk evaluation locations (coinciding with the 2018 Malawi census enumeration areas; see **Section 2.2**). On the other hand, **Figure 3b** shows the selected distribution types of the best-fitting upper-tail approximation models. The minimum correlation coefficients are above 0.999 at all locations. The best-fitting models are either Weibull or lognormal distribution. Using the simulation formulae (Equations (5) to (8)), the annual maximum PGA samples can be generated rapidly, and the simulated PGA values can be used for probabilistic seismic risk analysis. For interested readers, PSHA data, model coefficients of the approximated seismic hazard functions, and a MATLAB code for upper tail approximation are made available (see **Section 5**).

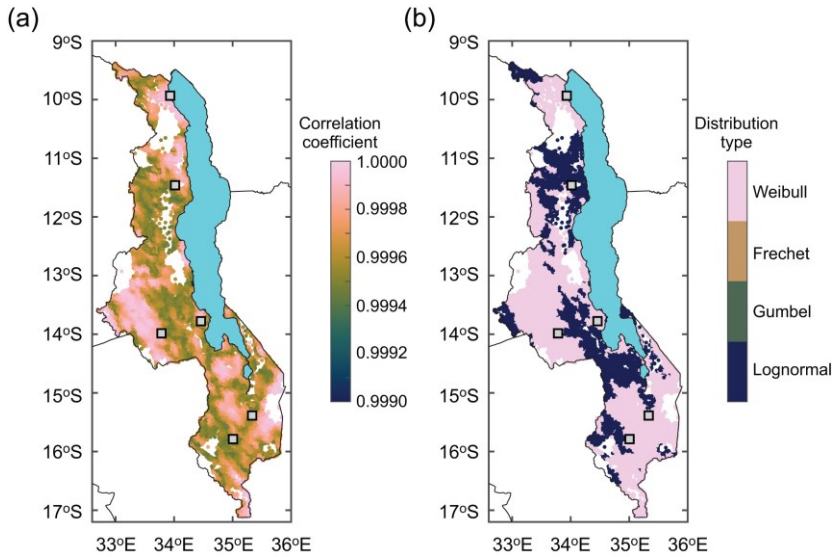

***Figure 3**. (a) Correlation coefficient of the PSHA data and the fitted upper tail approximation models. (b) Distribution type of the best fitting upper tail approximation models.*

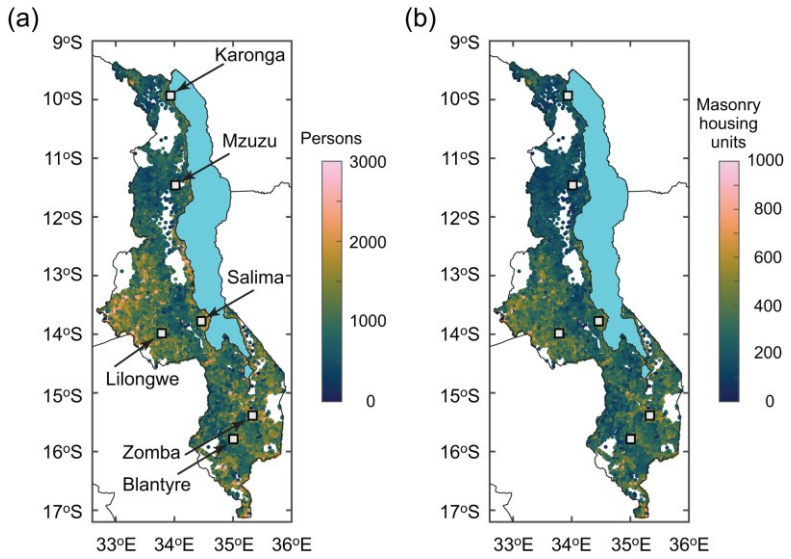

***Figure 4**. (a) Population map and (b) masonry building unit map based on Malawi census enumeration areas. The numbers are adjusted for the Year 2023.*

2.2. Masonry buildings in Malawi

Housing construction in Malawi has a crucial influence in determining the socioeconomic and financial impacts of earthquakes. Houses in local communities are one of the most vulnerable elements for a variety of reasons: (i) poor quality of construction materials, (ii) poor and variable construction practice, and (iii) lack of building design and construction provisions. The Malawi census is a reliable source of information on the current population and residential buildings in Malawi (National Statistical Office of Malawi, 2018). In the census,

existing dwellings are divided into three categories: (a) permanent (made of burnt clay bricks and iron sheet roofs), (b) semi-permanent (made of unburnt clay bricks and thatched roofs), and (c) traditional (made of rammed earth, daub and wattle or timber walls and lightweight thatched roofs). Out of 4,805,431 housing units listed in the 2018 census, 41.1% are permanent, 23.0% are semi-permanent, and 35.9% are traditional. 97% of the census surveyed dwellings can be considered as low-rise unreinforced constructions, consisting of owner/family occupied (85%), rented (12%), and institutional or other types (3%). The finest spatial administrative units of the census-based building data are enumeration areas. This study uses the enumeration areas for the spatial data resolutions of the seismic risk assessments. **Figures 4a** and **4b** show maps of the population and masonry building units at 18,714 enumeration areas. The numbers are adjusted for the Year 2023 from the Year 2018 by multiplying a factor of 1.192 (https://www.worldometers.info/world-population/malawi-population/).

2.3. Collapse fragility functions of masonry buildings in Malawi

Unreinforced masonry buildings in Malawi are vulnerable to seismic excitations. Kloukinas et al. (2020) conducted local building surveys in southern Malawi as part of the *PREPARE* project. A series of in-situ and laboratory tests were conducted to measure the strengths of typical construction materials in Malawi and to evaluate the in-plane and out-of-plane strengths of masonry wall panels (Voyagaki et al., 2020). Based on the gathered local data from the surveys and laboratory tests, Novelli et al. (2021) collected detailed geometrical and structural features of Malawian masonry buildings and applied a variant of the Failure Mechanism Identification and Vulnerability Evaluation (FaMIVE) method (D'Ayala and Speranza, 2003) to 646 surveyed façades for seismic vulnerability evaluations.

The seismic fragility functions developed by Novelli et al. (2021) distinguish buildings based on geometric and structural features into three vulnerability classes: A (poor-quality construction), B (medium-quality construction), and C (high-quality construction). The vulnerability class A is the most vulnerable, whereas the vulnerability class C is the least vulnerable. Typical buildings classified as vulnerability classes A, B and C are shown in **Figures 5a**, **5b**, and **5c**, respectively. Buildings with vulnerability class A are made of mud mortar combined with fired bricks of poor fabric quality and unfired bricks from poor to high fabric quality and have smaller building footprints than a typical floor plan of 8 m × 6 m (**Figure 5a**). Buildings with vulnerability class B are made of fired bricks characterized by poor to good quality fabric and have weak connections between walls due to the presence of mud mortar (**Figure 5b**). Buildings with vulnerability class C are made of fired bricks from poor to good quality fabric and cement mortar with the presence of strengthening elements (e.g., ring beams) and have larger floor plans than a typical plan of 8 m × 6 m (**Figure 5c**).

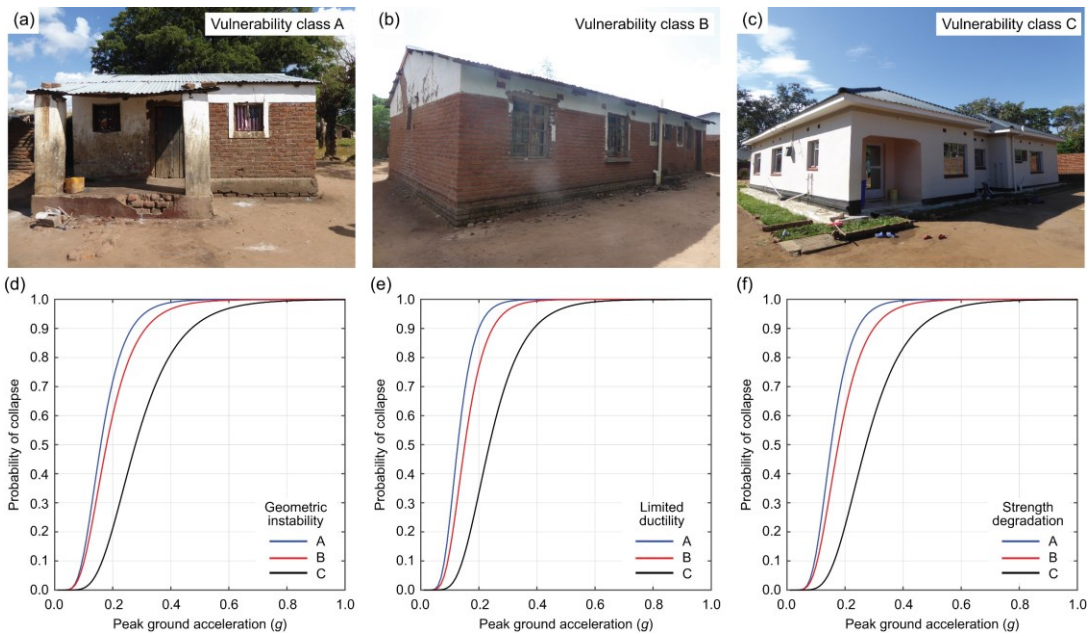

***Figure 5**. (a-c) Photos of typical masonry houses that are assigned with the vulnerability classes A, B, and C. (d-f) Collapse fragility functions for the vulnerability classes A, B, and C based on the geometric instability, limited ductility, and strength degradation as ultimate behavior in terms of building capacity curves.*

In developing seismic fragility functions of Malawian masonry buildings, three different types of ultimate (collapse) behavior in terms of building capacity curves (i.e., post-yield part of a force-displacement curve) are considered: geometric instability (D'Ayala and Paganoni, 2011), limited ductility (Lagomarsino, 2015), and strength degradation (Tomazevic, 2007). The geometric instability behavior and the strength degradation behavior consider three branches of a static pushover curve (with different definitions of the control points of the pushover curve), whereas the limited ductility behavior considers two branches of a static pushover curve without a plateau in the pushover curve. Since different ultimate behavior applies to vulnerability classes A, B, and C, nine applicable seismic fragility functions exist for the collapse limit state. The collapse fragility functions for the vulnerability classes A, B, and C by considering geometric instability, limited ductility, and strength degradation as ultimate behavior are shown in **Figures 5d**, **5e**, and **5f**, respectively. The input seismic intensity parameter for these collapse fragility functions is PGA, and the form of the collapse fragility function is the lognormal distribution. For the same ultimate behavior, buildings with the seismic vulnerability class A are more vulnerable (i.e., positioned towards the left-hand side of the figure), followed by those with the seismic vulnerability classes B and C, which is consistent with the building survey classifications. When the collapse fragility functions for different ultimate behavior are compared, those with limited ductility are more vulnerable than those with geometric instability or strength degradation. By assigning these nine collapse fragility functions to Malawian houses (**Section 2.2**; **Figure 4**), the seismic risk assessments can incorporate different building performances for the collapse limit states.

The final task of the exposure-vulnerability modules is to assign seismic fragility functions (**Figure 5**) to census building data, which are specified as permanent, semi-permanent, and traditional. The association of the collapse fragility functions and the census housing categories is conducted by reflecting the local knowledge and experiences gained through the building surveys and experiments conducted in Malawi. More specifically, FaMIVE-based collapse fragility functions with the vulnerability classes A, B, and C (**Figures 5d** to **5f**) are assigned to traditional, semi-permanent, and permanent buildings, respectively. Each vulnerability class has three possible ultimate behavioral patterns (i.e., geometrical instability, limited ductility, and strength degradation). The different ultimate behavior is considered to be equally likely.

2.4. Collapse risk assessment of masonry buildings in Malawi

With the site-specific seismic hazard curves in terms of the annual maximum PGA (**Section 2.1**) and the building collapse fragility functions (**Section 2.3**) for the census-based building inventory of masonry houses (**Section 2.2**), a building collapse risk curve for each building class (i.e., permanent, semi-permanent, and traditional) can be derived via Monte Carlo methods. More specifically, the following simulation steps can be implemented for each building location and type:

Step 1: Set the number of simulations N (e.g., 1 million samples with each representing a 1-year period).

Step 2: Extract the PSHA results for a site of interest (i.e., PGA values at the nine return period levels) and perform the upper tail approximation. Then, simulate N realizations of the annual maximum PGA.

Step 3: For individual annual maximum PGA values, evaluate the collapse probability of a building using a seismic fragility function.

Step 4: Post-processing of the results from *Step 3* can be presented as the collapse probability risk curve and collapse probability risk map.

When the numbers for individual building classes are available (e.g., **Figure 4**), the results can be used to calculate the number of collapsed buildings at each location, and these results can also be visualized in a map format. When the building cost information is available, the collapse risk assessment can be extended to seismic loss estimation, thereby facilitating the financial seismic risk analysis (note: this is outside of the current study's scope due to the lack of nationwide building cost information). It is important to emphasize that the collapse simulation based on the upper tail approximation is very fast because a full implementation of site-specific PSHA is circumvented. This allows the simulations of the building collapse risk over a large spatial region. To disseminate the developed seismic risk tool for Malawi, a MATLAB code for the collapse probability calculation is made available (see **Section 5**).

3. Application: Nationwide Assessment for Masonry Building Collapse Risk

3.1. Collapse risk assessment of masonry houses at a single location

Seismic hazard assessments in Malawi depend significantly on the fault source and ground motion models. Williams et al. (2023) considered 20 branches in the logic tree to capture the epistemic uncertainty. This uncertainty can be propagated to the building collapse risk assessments. **Figures 6a** to **6c** show the building collapse risk curves for a permanent house in Blantyre by considering 20 logic tree branches and by considering different seismic fragility functions with strength degradation, geometric instability, and limited ductility ultimate behavior. By comparing the three sub-figures in **Figures 6a** to **6c**, the effects of the seismic hazard characterizations and the ultimate collapse behavior of the permanent house can be examined. In Blantyre, due to the proximity to several local faults (**Figure 2a**), the influence of the fault-based seismic hazard characterization is more significant than that of the ultimate collapse behavior.

Figures 6d to **6f** show the variations of the collapse risk curves for different house types (permanent versus semi-permanent versus traditional) and for different ultimate collapse behavior patterns. The former corresponds to the differences in the collapse fragility functions for the vulnerability classes A, B, and C (**Figures 5d** to **5f**). It can be observed that the building classifications according to the vulnerability classes have significant impacts on the collapse risk curves. Overall, it is important to account for influences from seismic hazard uncertainty and seismic vulnerability uncertainty in the final building collapse risk assessments.

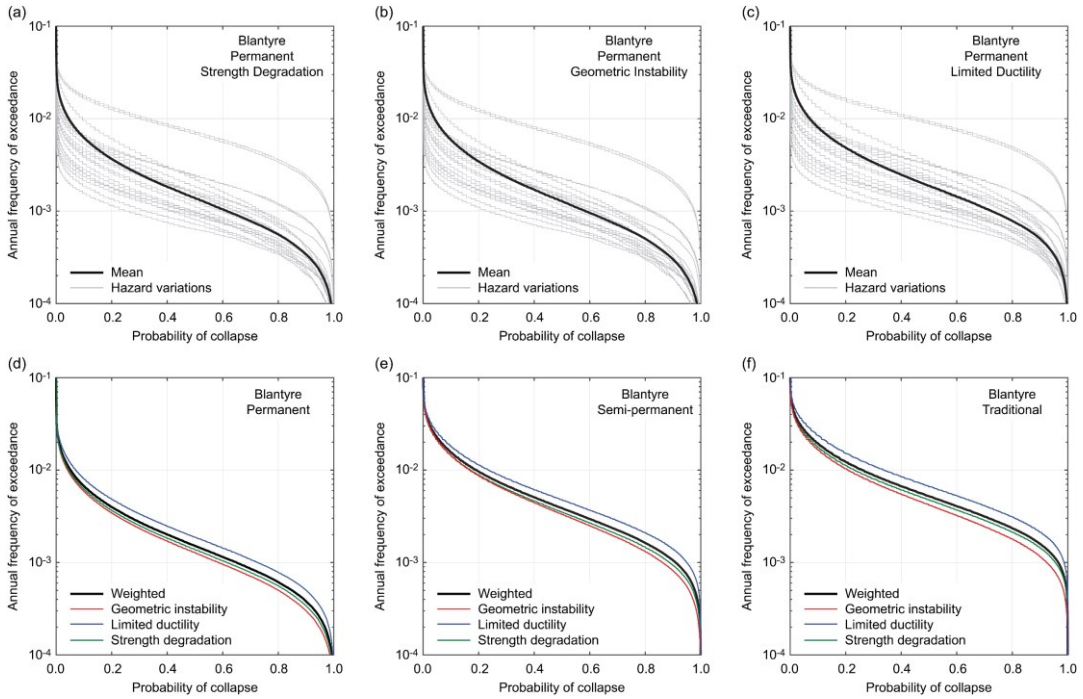

***Figure 6**. (a-c) Collapse probability curves of a permanent house in Blantyre based on 20 logic tree branches of seismic hazards by considering the strength degradation, geometric instability, and limited ductility ultimate behavior. (d-f) Collapse probability curves of permanent, semi-permanent, and traditional houses based on different ultimate behavior in terms of building capacity curves*.

3.2. Nationwide collapse risk assessment of masonry houses

National level collapse risk assessments can be carried out by repeating the collapse risk assessments for three types of masonry houses (i.e., permanent, semi-permanent, and traditional) in all census enumeration areas. **Figures 7a** to **7c** and **Figures 7d** to **7f** show the collapse probability maps of permanent, semi-permanent, and traditional houses corresponding to the return periods of 500 and 1,000 years, respectively. The PGA maps for the return periods of 500 and 1,000 years are shown in **Figures 2b** and **2c**, respectively. The results for the permanent house show that the collapse probability is high at locations near the major faults. Permanent houses away from Lake Malawi (e.g., near Lilongwe) do not have significant building collapse risks, whereas those near Karonga and north/south of Blantyre are associated with relatively large collapse risks. With the increase of the seismic vulnerability from class C (permanent) to A (traditional), the

high collapse risks prevail over a wide region near Lake Malawi and along the Shire River in southern Malawi. These high collapse risks can be understood by comparing the corresponding PGA maps (**Figures 2b** and **2c**) and the collapse fragility functions (**Figures 5d** to **5f**). Due to the anticipated poor seismic performance of semi-permanent and traditional houses in Malawi (which are mainly made of low-quality bricks with mud mortar and are not equipped with strengthening structural elements, such as ring beams and wall buttresses), the probability of building collapse increases rapidly when houses are subjected to PGA ≈ 0.15 *g* or greater. At the seismic hazard level of 500 to 1,000 years, most masonry houses are at significant risk due to structural collapse.

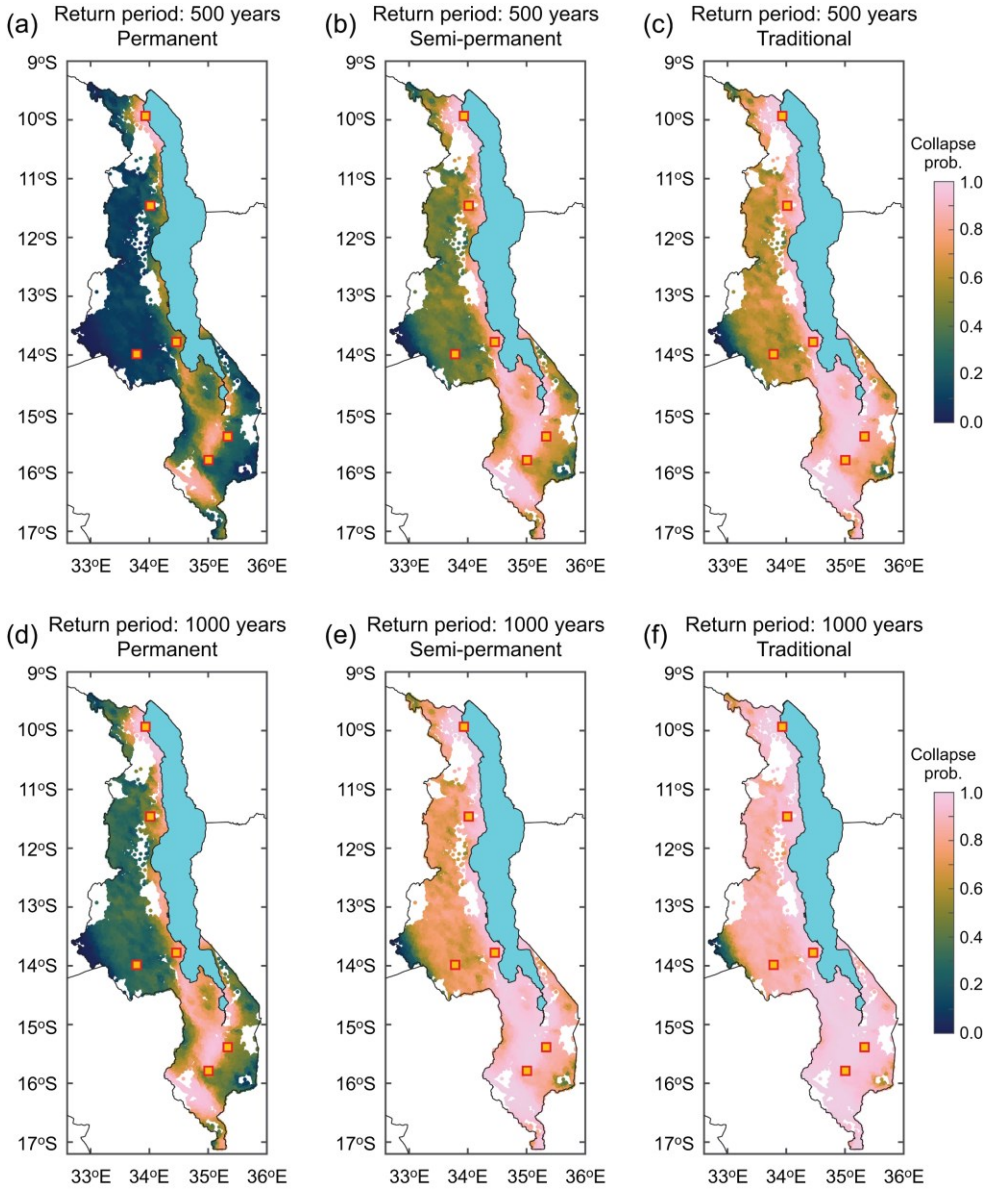

***Figure 7**. Collapse probability maps of the permanent, semi-permanent, and traditional houses corresponding to the return periods of 500 and 1,000 years.*

4. Conclusions

This study presented a nationwide seismic risk assessment tool and results for masonry houses in Malawi. The new seismic risk model incorporated the latest seismic hazard characterization of active faults in the southern segment of the East African Rift system and country-specific collapse fragility functions that apply to Malawian masonry constructions. The fault-based seismic hazard model reflects the current understanding of the fault sources and ground motion intensities for Malawi, and represent their uncertainties using 20 logic tree branches in the seismic hazard model. On the other hand, the bespoke collapse fragility functions for Malawi

have been derived based on local building surveys, experimental tests of local construction materials, and plausible failure mechanisms of the main structural elements of the Malawian houses. Overall, the new quantitative seismic risk model constitutes a significant improvement compared to those without country-specific hazard-exposure-vulnerability models.

The upper tail approximations of seismic hazard curves facilitated the seismic risk results. The collapse risk curves were derived for each building type and location by reflecting possible seismic hazard and vulnerability characteristics. Furthermore, the upper tail approximation method allowed the fast evaluations of building collapse risks at the national level, thereby informing emergency managers and policymakers of relative seismic risks in Malawi and of possible benefits of seismic strengthening (e.g., a change from the vulnerability class A to the vulnerability class C).

To facilitate the uptake of the new seismic hazard and risk assessment tools for Malawi, the computer codes and the obtained results (e.g., building collapse probability maps) are made available to interested readers and potential users (**Section 5**). The dissemination of the quantitative seismic risk decision-support tools is one of the goals of the *PREPARE* project.

5. Data and Code Availability

The data and MATLAB codes used in this article can be found at: https://github.com/KatsuGoda/PREPARE_MalawiRisk. In addition, a complete set of the PSHA model for Malawi, developed by Williams et al. (2023), can be found at: https://github.com/jack-williams1/Malawi_PSHA.

6. References

Akkar, S., Sandıkkaya, M.A., Bommer, J.J. (2014). Empirical ground-motion models for point- and extended-source crustal earthquake scenarios in Europe and the Middle East. *Bulletin of Earthquake Engineering*, 12: 359–387.

Atkinson, G.M., Adams, J. (2013). Ground motion prediction equations for application to the 2015 Canadian national seismic hazard maps. *Canadian Journal of Civil Engineering*, 40: 988–998.

Boore, D.M., Stewart, J.P., Seyhan, E., Atkinson, G.M. (2014). NGA-West2 equations for predicting PGA, PGV, and 5earthquakes. *Earthquake Spectra*, 30: 1057–1085.

Chiou, B.S.J., Youngs, R.R. (2014). Update of the Chiou and Youngs NGA model for the average horizontal component of peak ground motion and response spectra. *Earthquake Spectra*, 30: 1117–1153.

Cornell, C.A., Jalayer, F., Hamburger, R.O., and Foutch, D.A. (200 2). Probabilistic basis for 2000 SAC Federal Emergency Management Agency steel moment frame guidelines. *Journal of Structural Engineering*, 128: 526–533.

D'Ayala, D., Speranza, E. (2003). Definition of collapse mechanisms and seismic vulnerability of historic masonry buildings. *Earthquake Spectra*, 19, 479–509.

D'Ayala, D., Paganoni, S. (2011). Assessment and analysis of damage in L'Aquila historic city centre after 6th April 2009. *Bulletin of Earthquake Engineering*, 9: 81–104.

Flannery, J.W., Rosendahl, B.R. (1990). The seismic stratigraphy of Lake Malawi, Africa: implications for interpreting geological processes in lacustrine rifts. *Journal of African Earth Sciences (and the Middle East)*, 10: 519–548.

Goda, K., Novelli, V., De Risi, R., Kloukinas, P., Giordano, N., Macdonald, J., Kafodya, I., Ngoma, I., Voyagaki, E. (2022). Scenario-based earthquake risk assessment for central-southern Malawi: the case of the Bilila-Mtakataka fault. *International Journal of Disaster Risk Reduction*, 67: 102655.

Jackson, J., Blenkinsop, T. (1997). The Bilila-Mtakataka fault in Malawi: an active, 100-km long, normal fault segment in thick seismogenic crust. *Tectonics*, 16: 137–150.

Kloukinas, P., Kafodya, I., Ngoma, I., Novelli, V., Macdonald, J., Goda, K. (2020). A building classification scheme of housing stock in Malawi for earthquake risk assessment. *Journal of Housing and the Built Environment*, 35: 507–537.

Lagomarsino, S. (2015). Seismic assessment of rocking masonry structures. *Bulletin of Earthquake Engineering*, 13: 97–128.

Mitchell-Wallace, K., Jones, M., Hillier, J., Foote, M. (2017). *Natural Catastrophe Risk Management and Modelling: a Practitioner's Guide*, Wiley-Blackwell, 536 p.

National Statistical Office of Malawi (2018). *2018 Population and Housing Census*. Available at: http://www.nsomalawi.mw/index.php%3Foption%3Dcom_content%26view%3Darticle%26id%3D226:2018-malawi-population-and-housing-census%26catid%E2%80%89%3D%E2%80%898:reports%26Itemid%E2%80%89%3D%E2%80%896.

Novelli, V.I., De Risi, R., Ngoma, I., Kafodya, I., Kloukinas, P., Macdonald, J., Goda, K. (2021). Fragility curves for non-engineered masonry buildings in developing countries derived from real data based on structural surveys and laboratory tests. *Soft Computing*, 25: 6113–6138.

Poggi, V., Durrheim, R., Mavonga Tuluka, G., Weatherill, G., Gee, R., Pagani, M., Nyblade, A., Delvaux, D. (2017). Assessing seismic hazard of the East African Rift: a pilot study from GEM and AfricaArray. *Bulletin of Earthquake Engineering*, 15: 4499–4529.

Tomazevic, M. (2007). Damage as a measure for earthquake-resistant design of masonry structures: Slovenian experience. *Canadian Journal of Civil Engineering*, 34: 1403–1412.

Voyagaki, E., Kloukinas, P., Novelli, V., De Risi, R., Kafodya, I., Ngoma, I., Goda, K., and Macdonald, J. (2020). Masonry panel testing in Malawi. *Proceedings of the 17th World Conference on Earthquake Engineering*, Sendai, Japan, Paper C003152.

Wald, D.J., Allen, T.I. (2007). Topographic slope as a proxy for seismic site conditions and amplification. *Bulletin of the Seismological Society of America*, 97: 1379–1395.

Wedmore, L., Williams, J., Biggs, J., Fagereng, A., Mphepo, F., Dulanya, Z., Adams, B. A. (2020). Structural inheritance and border fault reactivation during active early-stage rifting along the Thyolo fault, Malawi. *Journal of Structural Geology*, 139: 104097.

Williams, J.N., Wedmore, L.N.J., Fagereng, A., Werner, M., Mdala, H., Shillington, D., Chindandali, P. (2022). Geologic and geodetic constraints on the magnitude and frequency of earthquakes along Malawi's active faults: the Malawi Seismogenic Source Model (MSSM). *Natural Hazards and Earth System Sciences*, 22(11), 3607–3639.

Williams, J.N., Werner, M.J., Goda, K., Wedmore, L.N.J., De Risi, R., Biggs, J., Mdala, H., Dulanya, Z., Fagereng, A. Mphepo, F., Chindandali, P. (2023). Fault-based probabilistic seismic hazard analysis in regions with low strain rates and a thick seismogenic layer: a case study from Malawi. *Geophysical Journal International*, 233: 2172–2206.